HHS Public Access

Author manuscript

Physiol Behav. Author manuscript; available in PMC 2023 April 01.

Published in final edited form as:

Physiol Behav. 2023 April 01; 262: 114105. doi:10.1016/j.physbeh.2023.114105.

Collateralizing ventral subiculum melanocortin 4 receptor circuits regulate energy balance and food motivation

Uday Singh[a], **Kenji Saito**[a], **Michael Z. Khan**[b], **Jingwei Jiang**[a], **Brandon A. Toth**[a], **Samuel R. Rodeghiero**[a], **Jacob E. Dickey**[a], **Yue Deng**[a], **Guorui Deng**[a], **Young-Cho Kim**[c], **Huxing Cui**[a,d,e,*]

[a]Department of Neuroscience and Pharmacology, University of Iowa Carver College of Medicine, Iowa City, IA, United States

[b]Department of Psychiatry, University of Iowa Carver College of Medicine, Iowa City, IA, United States

[c]Department of Neurology, University of Iowa Carver College of Medicine, Iowa City, IA, United States

[d]Iowa Neuroscience Institute, University of Iowa Carver College of Medicine, Iowa City, IA, United States

[e]F.O.E. Diabetes Research Center, University of Iowa Carver College of Medicine, Iowa City, IA, United States

Abstract

Hippocampal dysfunction is associated with major depressive disorder, a serious mental illness characterized by not only depressed mood but also appetite disturbance and dysregulated body weight. However, the underlying mechanisms by which hippocampal circuits regulate metabolic homeostasis remain incompletely understood. Here we show that collateralizing melanocortin 4 receptor (*MC4R*) circuits in the ventral subiculum (vSUB), one of the major output structures of the hippocampal formation, affect food motivation and energy balance. Viral-mediated cell type- and projection-specific input-output circuit mapping revealed that the nucleus accumbens shell (NAcSh)-projecting vSUB^{MC4R+} neurons send extensive collateral projections of to various hypothalamic nuclei known to be important for energy balance, including the arcuate, ventromedial and dorsomedial nuclei, and receive monosynaptic inputs mainly from the ventral CA1 and the anterior paraventricular nucleus of thalamus. Chemogenetic activation of NAcSh-projecting vSUB^{MC4R+}neurons lead to increase in motivation to obtain palatable food without noticeable effect on homeostatic feeding. Viral-mediated restoration of *MC4R* signaling in the

*Corresponding author at: Department of Neuroscience and Pharmacology, University of Iowa Carver College of Medicine, 51 Newton Road, 2-372 Bowen Science Building, Iowa City, IA 52242. huxing-cui@uiowa.edu (H. Cui).

Author contributions

HC contributed to conceptualization, data curation, formal analysis, funding acquisition, investigation, methodology, project administration, resources, software, supervision, validation and manuscript writing. US, KS, MZK, JJ, BAT, SRR, JED, YD and GD assisted the investigation, metholology, validation, and visualization. US, YK and HC contributed to the formal analysis. US, JJ and YK critically reviewed and edited the manuscript.

Supplementary materials

Supplementary material associated with this article can be found, in the online version, at doi:10.1016/j.physbeh.2023.114105.

vSUB partially restores obesity in *MC4R*-null mice without affecting anxiety- and depression-like behaviors. Collectively, these results delineate vSUB^{MC4R+} circuits to the unprecedented level of precision and identify the vSUB^{MC4R} signaling as a novel regulator of food reward and energy balance.

Keywords

Melanocortin 4 receptor; Ventral subiculum; Nucleus accumbens; Energy homeostasis; Food motivation; Major depressive disorder

1. Introduction

Hippocampal dysfunction has been implicated in the pathogenesis of major depressive disorder (MDD) [1,2], a serious mental illness characterized by not only depressed mood and anhedonia but also appetite disturbance and dysregulated body weight homeostasis [3–7]. Consistent with these symptoms associated with metabolic dysregulation, several molecular signaling pathways within the hippocampus have been reported to affect feeding, body weight and motivated behaviors [8–14]. These functional observations are further supported by neuroanatomical tract-tracing showing that neurons in the hippocampal formation densely innervate various brain regions involved in reward and metabolic regulation, including the nucleus accumbens (NAc) and the hypothalamus [15,16]. Most notable are the neurons in the ventral subiculum (vSUB), one of the major output structures of the hippocampal formation. Studies have shown that vSUB neurons densely innervate the NAc and the different hypothalamic nuclei known to be important for the regulation of metabolic homeostasis, including but not limited to the paraventricular nucleus of hypothalamus (PVN), the dorsomedial nucleus of hypothalamus (DMH), the ventromedial nucleus of hypothalamus (VMH) and the lateral hypothalamic area (LHA) [14, 17,18]. While some reports have also suggested collateral projections of vSUB neurons to different brain regions [14,16,19], a comprehensive understanding of these collateralizing circuits throughout the brain has not yet been achieved. Functionally, vSUB circuits have been implicated in motivated behavior, HPA axis regulation and stress responses [20]; however, whether these circuits also affect food reward and metabolic homeostasis remain unclear.

The brain melanocortin signaling pathway plays a key role in the regulation of energy metabolism [21,22]. The central melanocortin system consists of proopiomelanocortin (*POMC*)- and agouti-related peptide (*AgRP*)-expressing neurons in the arcuate nucleus of hypothalamus (ARC) and the neurons expressing melanocortin type 3 and 4 receptors (*MC3/4R*) across the brain. Small neuropeptides *AgRP* and *POMC*-derived α-melanocyte stimulating hormone (α-MSH) function as unique endogenous antagonist (or inverse agonist) and agonist for *MC3/4R*, respectively, to exert their biological effects. Extensive studies have shown that *MC4R* is a major mediator of the melanocortin system to regulate energy homeostasis, as genetic deficiency in the *MC4R* signaling pathway leads to early-onset obesity in both humans and rodents [23,24]. In contrast to highly localized expression of *AgRP* and *POMC* in the ARC, *MC4R* is widely expressed throughout the brain, including the different hypothalamic nuclei and extra-hypothalamic brain regions that are important

for reward and emotional behaviors, such as the prefrontal cortex, the amygdala and the hippocampal formation [25]. Consistent with widespread expression of *MC4Rs* in the limbic system, pharmacological studies have revealed that *MC4R* signaling also affects depression- and anxiety-like behaviors in rodents [26–29], although the brain regions mediating these effects remain unclear. In large contrast to the well-characterized hypothalamic *MC4R* circuits in feeding and energy homeostasis, very little is known about whether and how *MC4R* signaling pathways in those extra-hypothalamic brain regions contribute to metabolic physiology or emotional behaviors.

In the present study, we hypothesize that *MC4R* expression in vSUB neurons affect emotional behaviors, food reward and metabolic homeostasis through collateral projections to the NAc shell (NAcSh) and the different hypothalamic nuclei. We tested this hypothesis using an advanced viral-mediated cell type- and projection-specific input-output circuit mapping technique combined with circuit-specific functional chemogenetic approach as well as in vivo Cre/loxP gene manipulation system in mice.

2. Methods

2.1. Animals

MC4R-GFP BAC transgenic and Cre-dependently reactivatable *MC4R*-TB mice were generated and characterized as previously reported [25,30]. *MC4R*-2a-Cre knock-in mouse line [31] was originally obtained from Dr. Bradford Lowell group at Harvard University (Jackson Laboratory stock number 030,759). Mice were housed in the University of Iowa vivarium in a temperature-controlled environment (lights on: 06:00–18:00) with *ad lib* access to water and food. Both sexes of mature adult (20–24 weeks) mice were for neuroanatomical characterization (males) and chemogenetic experiment (females). Young adult (8–10 weeks) male MC4R-TB and WT littermates were used for functional investigation of vSUB MC4R signaling. All animal procedures were performed in accordance with the University of Iowa Institutional Animal Care and Use Committee guidelines.

2.2. Viral vectors

Different viral vectors from valid scientific vendors or created in the present study were used to comprehensively map the $vSUB^{MC4R+}$ circuits, including AAV2-GFP, AAV2-Cre-GFP and AAV-PHP.eB-DIO-eGFP (Addgene); Cre-dependent AAV-retro-DIO-Flp (Duke Viral Vector Core) and AAV2-DIO-MC4R-V5 (created in-house); Flp-dependent AAV8-fDIO–ChR2-eYFP (Salk Institute Viral Vector Core), AAV8-fDIOTVA-mCherry (Salk Institute Viral Vector Core), AAV8-fDIO-oG (Salk Institute Viral Vector Core), AAV2-fDIO-hM3Dq-mCherry (created in-house); and glycoprotein-deleted rabies virus (SADΔG-GFP, Salk Institute Viral Vector Core).

2.3. Stereotaxic surgery

Stereotactic surgery was performed as described in our previous publications [32–35]. Experimental procedures are also detailed in Supplemental Methods and Materials. The injection sites for every mouse that received stereotaxic microinjection were confirmed by

immunohistochemistry for GFP, mCherry, or V5 and miss-hit cases are excluded from the data analysis. At least three successfully targeted mice were included for each of neuroanatomical characterizations.

2.4. Immunohistochemistry (IHC)

IHC was performed as previously reported [32,35]. Briefly, the mice were transcardially perfused with 10% neutralized formalin and the brains were removed and immersed in 25% sucrose solution, cut into five series of 30 μm sections and stored in cryoprotectant at 20 °C until processed for IHC. Brain sections were rinsed in PBS, blocked in 3% normal donkey serum and 0.3% Triton X-100 in PBS for 30 min at room temperature. Sections were then incubated with primary antibodies against GFP (Aves Labs), mCherry (Clontech), c-Fos (CalBioChem), or V5 tag (Invitrogen) overnight at 4 °C, and then washed and incubated with Cy2-, Cy3- or Cy5-conjugated secondary antibodies (Jackson ImmunoResearch) for fluorescent visualization or with HRP-conjugated secondary antibody for chromogenic staining using an ABC kit as per the manufacturer's instructions (Vector Laboratories).

2.5. Food intake and body weight

For the chemogenetic study, *MC4R*-Cre^{+} mice ($n = 8$) were singly housed for 3–5 days prior to the feeding experiment. A crossover design was used for the testing. On the first day of testing, mice were divided into two groups ($n = 4$) and received IP injection of either saline or Clozapine-N-oxide (CNO, 2 mg/Kg) at the beginning of dark cycle (6 PM) in their home cages. Food intake was monitored at 4- and 24 h post-injection. The same experimental procedure was repeated the next day with crossover injection regimen.

For long-term feeding and body weight assessment, the *MC4R*-TB mice were housed either individually or in group after AAV injection into the vSUB and body weight was monitored weekly throughout the experimental period. Weekly food intake was also monitored in a singly housed cohort of *MC4R*-TB mice.

MTII-induced suppression of feeding was performed in singly housed *MC4R*-TB mice. The mice received IP injection of saline at the beginning of dark cycle (6 PM) and food intake was monitored at 2-, 4- and 24 h post-injection. On the next day, the same experimental procedure was repeated with IP injection of MTII (2 mg/Kg) instead of saline.

2.6. Behavioral tests

All behavioral tests were performed as described in our previous publications [35–37]. Experimental procedures are also detailed in Supplemental Methods and Materials. A crossover design was used for eight mice with chemogenetic activation of NAcSh-projecting vSUB^{MC4R+}neurons that were subjected to operant responding test for food motivation.

2.7. Statistical analyses

Statistical analyses were performed using GraphPad Prism (Graph-Pad Software, La Jolla, CA) software. Comparisons between groups were made by paired Student's *t*-test, one-way ANOVA or repeated measure two-way ANOVA with Tukey post hoc analysis as needed. $P < 0.05$ was considered statistically significant. Data are presented as mean ± SEM.

3. Results

3.1. MC4R is highly expressed in the vSUB

As a typical G protein-coupled receptor (GPCR), MC4R expression in the brain is extremely low and its detection has been technically challenging. BAC transgenic MC4R-GFP mouse model was generated to overcome this technical barrier and ease the detection of MC4R-expression cells, which revealed that in addition to the hypothalamic and brainstem nuclei, MC4Rs are also broadly expressed in the cortex, amygdala, and hippocampal formation, including the vSUB. However, there have been increasing concerns regarding whether a gene of interest is faithfully marked in BAC transgenic mice. Therefore, we generated triple transgenic mice bearing BAC MC4R-GFP, knock-in MC4R-Cre, and tdTomato reporter alleles and evaluated an overlapping nature of GFP (cells that currently express MC4R) and tdTomato (cells that currently express and/or have had transient MC4R expression during the development). Both GFP and tdTomato are highly expressed in the vSUB, confirming the MC4R expression in this brain region (Fig. 1A). While there is a considerable number of cells which co-express GFP and tdTomato, it is noteworthy that there are also some cells that express GFP but not tdTomato, or vice versa (Fig. 1A). In order to further evaluate true MC4R-expressing cells in the vSUB of adult mice, we injected Cre-dependent AAV-PHP.eB-DIO-eGFP directly into the lateral ventricle of adult MC4R-2a-Cre knock-in mouse [31] and examined eGFP expression in the vSUB. We observed a considerable number of GFP-expressing cells in the vSUB (Fig. 1B, C) in addition to the hypothalamic nuclei and other brain regions (data not shown), proving that many of vSUB neurons express MC4R in adult stage. Collectively, these qualitative neuroanatomical results confirm that many neurons in the vSUB of adult mice express MC4Rs.

3.2. NAcSh-projecting vSUB^{MC4R+} neurons send diffuse collateral projections to different brain regions

Neurons in the vSUB are known to project to multiple brain regions, including but not limited to, the NAcSh and the hypothalamus. Interestingly, bifurcating axonal projections of vSUB neurons to the septum and other brain regions have been reported [14,16,19]; however, whether vSUB^{MC4R+} neurons send collateral projections to the NAcSh and other brain regions remains unknown. To that end, we performed a slightly modified version of the cell type-specific tracing the relationship between input and output (cTRIO) technique [38] in *MC4R*-2a-Cre knock-in mice. We simultaneously injected retrogradely transporting AAV expressing Flp recombinase in Cre-dependent manner (AAV-retro-DIO-Flp) and AAV expressing ChR2-eYFP in Flp-dependent manner (AAV-fDIO–ChR2-eYFP) into the NAcSh and the vSUB of *MC4R*-Cre mice, respectively (Fig. 2A). After 4 weeks of microinjection, the mice were transcardially perfused and the brain sections were processed for FIHC for eYFP to identify additional brain regions receiving collateral projections from NAcSh-projecting vSUB^{MC4R+} neurons. This advanced cell type- and circuit-specific tract-tracing technique revealed that NAcSh-projecting vSUB^{MC4R+} neurons send substantial collateral projections to the VMH-capsule, the ventral part of lateral septal nucleus (LSV), the bed nucleus of stria terminalis (BNST), the medial preoptic nucleus (MPO), the ventrolateral preoptic nucleus (VLPO), the anterior paraventricular thalamic nucleus (PVA), the anterior hypothalamic area (AH), the dorsomedial nucleus of hypothalamus (DMH), the arcuate

nucleus of hypothalamus (ARC), the posterior nucleus of hypothalamic (PH), the medial amygdaloid nucleus (MeA), the basomedial amygdaloid nucleus (BMA), and the ventral tuberomammillary nucleus (VTM) (Fig. 2B). Sparse to moderate collateral projections were also observed in the medial prefrontal cortex (mPFC), the cingulate cortex (Cg), the lateral preoptic nucleus (LPO), the paraventricular nucleus of hypothalamus (PVH), the VMH-core, the retromammillary nucleus (RM), and the periaqueductal gray (PAG) (Fig. 2B). Zoom-in images in the ARC and DMH show eYFP puncta resembling synaptic boutons, indicating that these collateral hypothalamic projections may make functional synaptic connections to hypothalamic neurons which are important for feeding and metabolic regulation (Fig. 2C, D). The relative optical density of GFP fibers throughout the brain is evaluated in 3 successful cases and summarized in Fig. 2E.

3.3. MC4Rs do not localize to hypothalamic axon terminals of NAcSh-projecting vSUB^{MC4R+} neurons

Diffuse collateral projections of NAcSh-projecting vSUB^{MC4R+} neurons to different hypothalamic nuclei resemble the patterns of AgRP and α-MSH immunoreactivity [39,40], two unique neuropeptides function as endogenous ligands for *MC4R*. Because limited AgRP and POMC neuronal projections to the vSUB have been reported [39,40], we hypothesized that *MC4R*s in NAcSh-projecting vSUB^{MC4R+} neurons might be localized to their axon terminals distributed in different hypothalamic nuclei (Fig. 3A) and that AgRP and POMC neurons might synapse onto these *MC4R*-expressing axon terminals to affect vSUB→hypothalamus neurotransmission. To test this possibility, we created an AAV driving expression of C-terminal V5-tagged *MC4R* in a Cre-dependent manner (AAV-DIO-*MC4R*-V5) and stereotaxically injected it into the vSUB of *MC4R*-Cre mice (Fig. 3B). Despite correct targeting and considerable expression of *MC4R*-V5 in vSUB^{MC4R+} neurons confirmed by V5 FIHC (Fig. 3C), we did not observe V5 FIHC signals in the hypothalamus (Fig. 3D). We also performed a control experiment to prove that MC4Rs can be localized in axon terminals. We injected AAV-DIO-MC4R-V5 into the PVN of MC4R-Cre mice (Fig. 3E) and evaluated axon terminal localization of MC4Rs in the median eminence (ME) based on our recent finding that PVN MC4R+ neurons heavily innervate the ME [41], which revealed that at least in PVN MC4R+ neurons, MC4Rs can be localized to axon terminals within the ME in addition to somatic/dendritic expression (Fig. 3F, G).

3.4. Brain-wide mapping of monosynaptic inputs to NAcSh-projecting vSUB^{MC4R+} neurons

cTRIO technique enables the unbiased mapping of brain regions where neurons send monosynaptic inputs to a genetically defined group of neurons that project to a specific brain region. Using cTRIO, we mapped the brain regions where neurons provide monosynaptic inputs to NAcSh-projecting vSUB^{MC4R+} neurons. We simultaneously injected AAV-retro-DIO-Flp into the NAcSh and AAVs expressing rabies glycoprotein (RG) and cognate receptor (TVA-mCherry) for avian virus envelope glycoprotein (EnvA) in Flp-dependent manner (AAV-fDIO-RG and AAV-fDIO-TVA-mCherry) into the vSUB of *MC4R*-Cre mice (Fig. 4A). After 3 weeks of viral injection, EnvA-pseudotyped G-deleted-eGFP rabies virus (SADΔG-GFP) was injected into the vSUB to label neurons providing monosynaptic inputs to NAcSh-projecting vSUB^{MC4R+} neurons (Fig. 4A). Double FIHC revealed an overlapping

expression of mCherry and GFP in vSUB, indicating the precise stereotaxic targeting (Fig. 4B). Subsequent examination of GFP+ cells revealed relatively limited distribution of GFP+ cells throughout the whole brain. Notable brain regions containing GFP+ cells include the vertical limb of the diagonal band (VDB), the PVA, the amygdalo-hippocampal transition area (AHiPM), and CA1 region of ventral hippocampus (vCA1) (Fig. 4C, D). A limited number of GFP+ cells were also observed in the medial septum (MS), the ARC and the dorsal raphe nucleus (DRN) (Fig. 4C, D).

3.5. Chemogenetic activation of NAcSh-projecting vSUB^{MC4R+} neurons affect appetitive motivation for palatable food

After cTRIO-mediated circuit mapping which revealed dense collateral projections of vSUB^{MC4R+}neurons to the NAcSh and various hypothalamic nuclei, we tested the role of these collateralizing vSUB^{MC4R} circuits in homeostatic feeding and appetitive motivation for palatable food using the designer receptor exclusively activated by designer drugs (DREADD) approach. For this circuit-specific chemogenetic approach, we simultaneously injected AAV-retro-DIO-Flp into the NAcSh and AAV expressing excitatory DREADD receptor hM3Dq-mCherry in Flp-dependent manner (AAV-fDIO-hM3Dq-mCherry) into the vSUB of *MC4R*-Cre mice (Fig. 5A), which allows expression of excitatory DREADD receptor hM3Dq exclusively in NAcSh-projecting vSUB^{MC4R+} neurons (Fig. 5B). Intraperitoneal (IP) injection of otherwise inert small molecule ligand, Clozapine-N-oxide (CNO, 2 mg/Kg) resulted in activation of NAcSh-projecting vSUB^{MC4R+}neurons as assessed by double FIHC for mCherry and c-Fos, an established marker of neuronal activation (Fig. 5C, D). No c-Fos induction was observed in any of those vSUB$^{mCherry+}$ neurons when mice were received IP injection of saline (data not shown). Subsequent behavioral assessments with crossover experimental design revealed that DREADD activation of these collateralizing vSUB^{MC4R+} circuits right before dark cycle (5 PM) does not significantly affect homeostatic feeding (Fig. 5E). Since the NAcSh is well known to regulate food motivation, we trained these mice in an operant responding box to press the lever for palatable high-sucrose food pellets to test appetitive motivation for palatable food. Once the mice successfully pass the required fixed-ratio (FR) training schedule, we divided overnight fasted mice into two groups (n = 4/group) and subject them to 2-day progressive-ratio (PR) test for appetitive motivation with crossover injection regimen. Interestingly, DREADD activation of these collateralizing vSUB^{MC4R+} circuits significantly increased the number of lever presses, the breakpoint, and the numbers of food reward earned during PR test (Fig. 5F–H), indicating heightened appetitive motivation for palatable food.

3.6. Restoration of MC4R signaling specifically in the vSUB of obese MC4R-null mice suppress body weight and food intake

While cell type- and projection-specific DREADD approach provided novel insight into the role of vSUB^{MC4R+} circuits in feeding and food motivation, the experimental outcomes from DREADD approach do not prove the role of *MC4R* signaling per se. In order to further clarify the physiological role of vSUB^{MC4R} signaling, we used a genetically engineered *MC4R*-null mouse model enabling Cre-dependent re-expression of endogenous *MC4R*s (*MC4R*-TB), which we have successfully used in our previous study to restore *MC4R* expression in the LHA using AAV-Cre-GFP [34]. Around 10-week of age, we performed

bilateral stereotaxic injection to deliver AAV-Cre-GFP or AAV-GFP into the vSUB of obese *MC4R*-TB mice to restore endogenous *MC4R* expression specifically in the vSUB (Fig. 6A, B). Weekly measurement of body weight in group-housed mice revealed that restoration of vSUB^{MC4R} signaling significantly suppress weight gain in obese *MC4R*-TB mice (Fig. 6C). In order to repeat this interesting observation and to evaluate the role of vSUB^{MC4R} signaling in homeostatic feeding, we prepared another cohort of *MC4R*-TB mice and performed viral injection at the 8-week of age and singly housed them throughout the experimental period. Continuous weekly measurement of body weight again revealed a significantly suppressed weight gain in *MC4R*-TB mice that received AAV-Cre-GFP injection into the vSUB compared to littermates *MC4R*-TB mice that received AAV-GFP injection (Fig. 6D). Weekly food intake was significantly higher in *MC4R*-TB compared to WT littermates as expected, and although not statistically significant, there was a strong trend toward reduced food intake in *MC4R*-TB mice that received AAV-Cre-GFP injection into the vSUB (Fig. 6E, F). We also performed an acute pharmacological experiment in these mice to evaluate the anorectic response to the synthetic *MC3/4R* agonist, melanotan II (MTII). *MC4R*-TB mice exhibited blunted anorectic response to MTII compared to WT littermates as expected, which is partially normalized by restoration of vSUB^{MC4R} signaling exclusively in the vSUB (Fig. 6G, H). Home cage behaviors measured by the LABORAS system revealed that *MC4R*-TB mice have reduced locomotor activity, which was partially rescued by the restoration of vSUB^{MC4R} signaling (Fig. 6I). *MC4R*-TB mice also showed decreased climbing and increased grooming, which were not rescued by the restoration of vSUB^{MC4R} signaling (Fig. 6I).

3.7. Restoration of vSUB MC4R signaling does not affect anxiety- and depression-like behaviors

Because of the well-known role of the hippocampus in emotional regulation, we also subjected the mice to different behavioral paradigms measuring anxiety- and depression-like behaviors. Behavioral tests were performed after 3 weeks of AAV-Cre-GFP injection into the vSuB of MC4R-TB mice. In contrast to previous pharmacological studies, we did not observe any anxiety- (Fig. 7A–C) or depression-like (Fig. 7D–F) behaviors in obese *MC4R*-TB mice that received microinjection of either AAV-GFP or AAV-Cre-GFP into the vSUB.

4. Discussion

Accumulating evidence support a role for the hippocampus to affect feeding and body weight regulation [42–44]. Despite abundant expression of *MC4Rs* in the hippocampal formation [25,45], it has been unclear whether and how hippocampal *MC4R* circuits contribute to these physiological processes. In present study, we discovered that vSUB^{MC4R} circuits affect food motivation and long-term energy balance.

Using an innovative cTRIO technique [38], we were able to decode the complex axonal collateralizations of NAcSh-projecting vSUB^{MC4R+} neurons as well as monosynaptic inputs to this anatomically and molecularly defined subgroup of vSUB^{MC4R+} neurons, furthering the understanding of the neuroanatomical basis of vSUB^{MC4R+} circuits for these behavioral

and physiological regulations. The existence of collateral projections of vSUB neurons has been reported [14,16,19], although a recent study utilizing a viral-mediated approach has challenged this view [18]. Our results from more advanced cell type- and projection-specific circuit mapping, however, strongly indicate that axonal collateralization is a common feature for vSUB neurons, at least for NAcSh-projecting vSUB^{MC4R+} neurons. Brain-wide mapping of monosynaptic inputs to NAcSh-projecting vSUB^{MC4R+} neurons revealed that, in addition to expected heavy inputs from vCA1 neurons, considerable monosynaptic inputs to NAcSh-projecting vSUB^{MC4R+} neurons are also originating from neurons residing in the PVA. Since the PVA also receives dense inputs from vSUB^{MC4R+} neurons (Fig. 2E), it is of great interest for future studies to clarify the role of reciprocal connections between the PVA and vSUB^{MC4R+} neurons in the regulation of food reward and energy balance. Although viral mediated approach has become a popular tool for neural circuit mapping, we do acknowledge some technical limitations for the neuroanatomical characterization carried out in the present study. For instance, both cell type- and projection-specific anterograde and retrograde monosynaptic tracing performed in the present study rely on the use of AAV-retro-DIO-Flp in MC4R-Cre mice for subsequent Cre-lox and Flp-FRT double recombination; however, the efficacy of double recombination could be much lower than originally thought, which might have underestimated the actual neuroanatomical organization of vSUB^{MC4R+} neurons. Additionally, the expression levels of glycoprotein (G) and TVA on the target neuron and the titer of SADΔG-GFP seem to be critical for the efficient labeling of monosynaptic input neurons [46]; however, in the present study, we did not test different titer and/or volume for these viral vectors for optimal use, which may have caused insufficient labeling of monosynaptic input neurons. Keeping these technical limitations in mind will help to avoid a potential misinterpretation of neuroanatomical observations in the present study.

A previous whole-brain mapping study failed to detect *AgRP* and α-MSH immunoreactivity in the vSUB [39], which is somewhat consistent with a recent viral-mediated circuit mapping showing minimal projections of both AgRP and POMC neurons to the vSUB [40]. Thus, it is less likely that vSUB^{MC4R+} neurons sense AgRP and α-MSH ligand neuropeptides via synaptic inputs from the ARC neurons. An electrophysiological study indicated a possible presynaptic action of *MC4R*s [47]; however, our viral-mediated overexpression of V5-tagged *MC4R*s in vSUB^{MC4R+} neurons does not support this idea. Another possibility is that POMC-derived small neuropeptides (including α-MSH) found in the cerebrospinal fluid (CSF) [48–50] could be the source of ligand for vSUB^{MC4R}s.

We consistently observed a significantly suppressed body weight gain by selective restoration of vSUB^{MC4R} signaling in two independent cohorts of obese *MC4R*-TB mice housed either singly or in group. While the trend toward reduced weekly food intake is likely the cause of reduced body weight, our results do not rule out the possibility that energy expenditure (EE) might have also contributed to this phenotype, as heavy innervations of vSUB^{MC4R+} neurons are observed in the MPA, VMH and DMH— brain nuclei that all have been strongly implicated in thermoregulation and EE [51–53]; or it could be the result of a combination of marginally decreased food intake and increased EE. In agreement with a recent study showing the moderate monosynaptic inputs from the vSUB neurons to both POMC and AgRP neurons (more so to POMC neurons) [40], we observed

the considerable collateral projections of NAcSh-projecting vSUB^{MC4R+} neurons to the ARC. It is of great interest for future studies to determine whether this novel vSUB→ARC monosynaptic circuit contributes to homeostatic regulation of energy balance.

The role of vSUB circuits in appetitive motivation for drug reward has been well documented [54], although less is known its role in food motivation. We observed an increase in motivation for palatable food by DRADD activation of NAcSh-projecting vSUB^{MC4R+} neurons without apparent changes in homeostatic feeding. It is noteworthy that neural substrates regulating homeostatic feeding versus food motivation could be substantially different. For example, we have previously shown that MC4R-TB mice have significantly reduced motivation to work for palatable food in PR test despite being hyperphagic when food is readily available under normal housing condition [55], indicating an important but opposing role of MC4R signaling in homeostatic feeding and food motivation upon calorie depletion. Activation of NAcSh neurons has long been known to elicit hedonic feeding in satiated animals [56]. Since NAcSh-projecting vSUB neurons are largely glutamatergic, the increased appetitive motivation could be due to augmented vSUB^{MC4R+}→NAcSh glutamatergic neurotransmission, although we cannot rule out the possibility that collateral projections to other brain regions, such as the mPFC and the LSV, may have also contributed to increased appetitive motivation for palatable food. Future site-specific optogenetic stimulation studies are needed to test this possibility.

Despite previous pharmacological studies revealing a role for *MC4R* signaling in anxiety- and depression-like behaviors in rodents [26–29], the genetic mouse model of *MC4R* deficiency used in the present study does not support a role for *MC4R* signaling in the regulation of anxiety-or depression-like behaviors. However, caution is also needed for this conclusion because behavioral performance could be hampered in *MC4R*-TB mice due to severe obesity. Future behavioral studies in mice with selective deletion of vSUB^{MC4Rs} are needed to clarify whether vSUB^{MC4R} signaling is required for the regulation of anxiety- and depression-like behaviors.

5. Conclusion

In conclusion, we have discovered vSUB^{MC4R} signaling as a novel regulator of food motivation and long-term energy balance and delineated the underlying neural circuits to the unprecedented level of precision. These findings further the understanding of how hippocampal formation affects food reward and energy balance, which may help to develop a novel strategy to prevent or treat appetite disturbance and dysregulated body weight in patients with MDD by safely targeting brain *MC4R* signaling.

Supplementary Material

Refer to Web version on PubMed Central for supplementary material.

Acknowledgments

We would like to thank Drs. Joel Elmquist (UT Southwestern Medical Center, Dallas, TX) and Bradford Lowell (Beth Israel Deaconess Medical Center, Boston, MA) for the use of *MC4R*-GFP, *MC4R*-Cre, and *MC4R*-TB mouse

lines. This work was supported by grants from the National Institutes of Health (HL127673, MH109920 and HL153274 to HC) and the American Heart Association (14SDG20140054 to HC).

References

[1]. Boku S, Nakagawa S, Toda H, Hishimoto A, Neural basis of major depressive disorder: beyond monoamine hypothesis, Psychiatry Clin. Neurosci 72 (1) (2018) 3–12. [PubMed: 28926161]

[2]. Malykhin NV, Coupland NJ, Hippocampal neuroplasticity in major depressive disorder, Neuroscience 309 (2015) 200–213. [PubMed: 25934030]

[3]. Milaneschi Y, Simmons WK, van Rossum EFC, Penninx BW, Depression and obesity: evidence of shared biological mechanisms, Mol. Psychiatry 24 (1) (2019) 18–33. [PubMed: 29453413]

[4]. Treadway MT, Zald DH, Reconsidering anhedonia in depression: lessons from translational neuroscience, Neurosci. Biobehav. Rev 35 (3) (2011) 537–555. [PubMed: 20603146]

[5]. Simmons WK, Burrows K, Avery JA, Kerr KL, Bodurka J, Savage CR, et al. , Depression-related increases and decreases in appetite: dissociable patterns of aberrant activity in reward and interoceptive neurocircuitry, Am. J. Psychiatry 173 (4) (2016) 418–428. [PubMed: 26806872]

[6]. Baxter LC, Appetite changes in depression, Am. J. Psychiatry 173 (4) (2016) 317–318. [PubMed: 27035529]

[7]. Merikangas AK, Mendola P, Pastor PN, Reuben CA, Cleary SD, The association between major depressive disorder and obesity in US adolescents: results from the 2001–2004 National Health and Nutrition Examination Survey, J. Behav. Med 35 (2) (2012) 149–154. [PubMed: 21479835]

[8]. Suarez AN, Liu CM, Cortella AM, Noble EE, Kanoski SE, Ghrelin and orexin interact to increase meal size through a descending hippocampus to hindbrain signaling pathway, Biol. Psychiatry (2019).

[9]. Hsu TM, Hahn JD, Konanur VR, Lam A, Kanoski SE, Hippocampal GLP-1 receptors influence food intake, meal size, and effort-based responding for food through volume transmission, Neuropsychopharmacology 40 (2) (2015) 327–337. [PubMed: 25035078]

[10]. Kanoski SE, Grill HJ, Hippocampus contributions to food intake control: mnemonic, neuroanatomical, and endocrine mechanisms, Biol. Psychiatry 81 (9) (2017) 748–756. [PubMed: 26555354]

[11]. Hsu TM, Hahn JD, Konanur VR, Noble EE, Suarez AN, Thai J, et al. , Hippocampus ghrelin signaling mediates appetite through lateral hypothalamic orexin pathways, Elife 4 (2015).

[12]. Hsu TM, Noble EE, Liu CM, Cortella AM, Konanur VR, Suarez AN, et al. , A hippocampus to prefrontal cortex neural pathway inhibits food motivation through glucagon-like peptide-1 signaling, Mol. Psychiatry 23 (7) (2018) 1555–1565. [PubMed: 28461695]

[13]. Kanoski SE, Hayes MR, Greenwald HS, Fortin SM, Gianessi CA, Gilbert JR, et al. , Hippocampal leptin signaling reduces food intake and modulates food-related memory processing, Neuropsychopharmacology 36 (9) (2011) 1859–1870. [PubMed: 21544068]

[14]. LeGates TA, Kvarta MD, Tooley JR, Francis TC, Lobo MK, Creed MC, et al. , Reward behaviour is regulated by the strength of hippocampus-nucleus accumbens synapses, Nature 564 (7735) (2018) 258–262. [PubMed: 30478293]

[15]. Kelley AE, Domesick VB, The distribution of the projection from the hippocampal formation to the nucleus accumbens in the rat: an anterograde- and retrograde-horseradish peroxidase study, Neuroscience 7 (10) (1982) 2321–2335. [PubMed: 6817161]

[16]. Namura S, Takada M, Kikuchi H, Mizuno N, Topographical organization of subicular neurons projecting to subcortical regions, Brain Res. Bull 35 (3) (1994) 221–231. [PubMed: 7812801]

[17]. Kishi T, Tsumori T, Ono K, Yokota S, Ishino H, Yasui Y, Topographical organization of projections from the subiculum to the hypothalamus in the rat, J. Comp. Neurol 419 (2) (2000) 205–222. [PubMed: 10722999]

[18]. Wee RWS, MacAskill AF, Biased connectivity of brain-wide inputs to ventral subiculum output neurons, Cell Rep 30 (11) (2020) 3644–3654, e3646. [PubMed: 32187537]

[19]. Swanson LW, Sawchenko PE, Cowan WM, Evidence for collateral projections by neurons in Ammon's horn, the dentate gyrus, and the subiculum: a multiple retrograde labeling study in the rat, J. Neurosci 1 (5) (1981) 548–559. [PubMed: 6180146]

[20]. O'Mara SM, Commins S, Anderson M, Gigg J, The subiculum: a review of form, physiology and function, Prog. Neurobiol 64 (2) (2001) 129–155. [PubMed: 11240210]

[21]. Myers MG Jr., Olson DP, Central nervous system control of metabolism, Nature 491 (7424) (2012) 357–363. [PubMed: 23151578]

[22]. Kleinridders A, Konner AC, Bruning JC, CNS-targets in control of energy and glucose homeostasis, Curr. Opin. Pharmacol 9 (6) (2009) 794–804. [PubMed: 19884043]

[23]. Farooqi IS, Monogenic human obesity, Front. Horm. Res 36 (2008) 1–11. [PubMed: 18230891]

[24]. Cone RD, Anatomy and regulation of the central melanocortin system, Nat. Neurosci 8 (5) (2005) 571–578. [PubMed: 15856065]

[25]. Liu H, Kishi T, Roseberry AG, Cai X, Lee CE, Montez JM, et al. , Transgenic mice expressing green fluorescent protein under the control of the melanocortin-4 receptor promoter, J. Neurosci 23 (18) (2003) 7143–7154. [PubMed: 12904474]

[26]. Sabban EL, Serova LI, Alaluf LG, Laukova M, Peddu C, Comparative effects of intranasal neuropeptide Y and HS014 in preventing anxiety and depressive-like behavior elicited by single prolonged stress, Behav. Brain Res 295 (2015) 9–16. [PubMed: 25542511]

[27]. Chaki S, Okubo T, Sekiguchi Y, Non-monoamine-based approach for the treatment of depression and anxiety disorders, Recent Pat. CNS Drug Discov 1 (1) (2006) 1–27. [PubMed: 18221188]

[28]. Chaki S, Okuyama S, Involvement of melanocortin-4 receptor in anxiety and depression, Peptides 26 (10) (2005) 1952–1964. [PubMed: 15979204]

[29]. Lim BK, Huang KW, Grueter BA, Rothwell PE, Malenka RC, Anhedonia requires MC4R-mediated synaptic adaptations in nucleus accumbens, Nature 487 (7406) (2012) 183–189. [PubMed: 22785313]

[30]. Balthasar N, Dalgaard LT, Lee CE, Yu J, Funahashi H, Williams T, et al. , Divergence of melanocortin pathways in the control of food intake and energy expenditure, Cell 123 (3) (2005) 493–505. [PubMed: 16269339]

[31]. Garfield AS, Li C, Madara JC, Shah BP, Webber E, Steger JS, et al. , A neural basis for melanocortin-4 receptor-regulated appetite, Nat. Neurosci 18 (6) (2015) 863–871. [PubMed: 25915476]

[32]. Cui H, Sohn JW, Gautron L, Funahashi H, Williams KW, Elmquist JK, et al. , Neuroanatomy of melanocortin-4 receptor pathway in the lateral hypothalamic area, J. Comp. Neurol 520 (18) (2012) 4168–4183. [PubMed: 22605619]

[33]. Vialou V, Cui H, Perello M, Mahgoub M, Yu HG, Rush AJ, et al. , A role for DeltaFosB in calorie restriction-induced metabolic changes, Biol. Psychiatry 70 (2) (2011) 204–207. [PubMed: 21215388]

[34]. Morgan DA, McDaniel LN, Yin T, Khan M, Jiang J, Acevedo MR, et al. , Regulation of glucose tolerance and sympathetic activity by MC4R signaling in the lateral hypothalamus, Diabetes 64 (6) (2015) 1976–1987. [PubMed: 25605803]

[35]. Cui H, Lu Y, Khan MZ, Anderson RM, McDaniel L, Wilson HE, et al. , Behavioral disturbances in estrogen-related receptor alpha-null mice, Cell Rep. 11 (3) (2015) 344–350. [PubMed: 25865889]

[36]. Lutter M, Khan MZ, Satio K, Davis KC, Kidder IJ, McDaniel L, et al. , The eating-disorder associated HDAC4(A778T) mutation alters feeding behaviors in female mice, Biol. Psychiatry 81 (9) (2017) 770–777. [PubMed: 27884425]

[37]. Davis KC, Saito K, Rodeghiero SR, Toth BA, Lutter M, Cui H, Behavioral alterations in mice carrying homozygous HDAC4 (A778T) missense mutation associated with eating disorder, Front. Neurosci 14 (2020) 139. [PubMed: 32153359]

[38]. Schwarz LA, Miyamichi K, Gao XJ, Beier KT, Weissbourd B, DeLoach KE, et al. , Viral-genetic tracing of the input-output organization of a central noradrenaline circuit, Nature 524 (7563) (2015) 88–92. [PubMed: 26131933]

[39]. Bagnol D, Lu XY, Kaelin CB, Day HE, Ollmann M, Gantz I, et al. , Anatomy of an endogenous antagonist: relationship between Agouti-related protein and proopiomelanocortin in brain, J. Neurosci 19 (18) (1999) RC26. [PubMed: 10479719]

[40]. Wang D, He X, Zhao Z, Feng Q, Lin R, Sun Y, et al. , Whole-brain mapping of the direct inputs and axonal projections of POMC and AgRP neurons, Front. Neuroanat 9 (2015) 40. [PubMed: 25870542]

[41]. Singh U, Jiang J, Saito K, Toth BA, Dickey JE, Rodeghiero SR, et al. , Neuroanatomical organization and functional roles of PVN MC4R pathways in physiological and behavioral regulations, Mol Metab 55 (2022) 101401. [PubMed: 34823066]

[42]. Liu CM, Kanoski SE, Homeostatic and non-homeostatic controls of feeding behavior: distinct vs. common neural systems, Physiol. Behav 193 (Pt B) (2018) 223–231. [PubMed: 29421588]

[43]. Stevenson RJ, Francis HM, The hippocampus and the regulation of human food intake, Psychol. Bull 143 (10) (2017) 1011–1032. [PubMed: 28616995]

[44]. Sweeney P, Yang Y, Neural circuit mechanisms underlying emotional regulation of homeostatic feeding, Trends Endocrinol. Metab 28 (6) (2017) 437–448. [PubMed: 28279562]

[45]. Kishi T, Aschkenasi CJ, Lee CE, Mountjoy KG, Saper CB, Elmquist JK, Expression of melanocortin 4 receptor mRNA in the central nervous system of the rat, J. Comp. Neurol 457 (3) (2003) 213–235. [PubMed: 12541307]

[46]. Cowley MA, Pronchuk N, Fan W, Dinulescu DM, Colmers WF, Cone RD, Integration of NPY AGRP, and melanocortin signals in the hypothalamic paraventricular nucleus: evidence of a cellular basis for the adipostat, Neuron 24 (1) (1999) 155–163. [PubMed: 10677034]

[47]. De Rotte AA, Verhoef J, Andringa-Bakker EA, Van Wimersma Greidanus TB, Characterization of the alpha-MSH-like immunoreactivity in blood and cerebrospinal fluid of the rat, Acta Endocrinol. (Copenh) 111 (4) (1986) 440–444. [PubMed: 3705883]

[48]. Pritchard LE, Oliver RL, McLoughlin JD, Birtles S, Lawrence CB, Turnbull AV, et al. , Proopiomelanocortin-derived peptides in rat cerebrospinal fluid and hypothalamic extracts: evidence that secretion is regulated with respect to energy balance, Endocrinology 144 (3) (2003) 760–766. [PubMed: 12586751]

[49]. Jackson S, Kiser S, Corder R, Lowry PJ, Pro-opiocortin peptides in rat cerebrospinal fluid, Regul. Pept 11 (2) (1985) 159–171. [PubMed: 2994177]

[50]. Morrison SF, Madden CJ, Tupone D, Central neural regulation of brown adipose tissue thermogenesis and energy expenditure, Cell Metab. 19 (5) (2014) 741–756. [PubMed: 24630813]

[51]. Munzberg H, Qualls-Creekmore E, Berthoud HR, Morrison CD, Yu S, Neural control of energy expenditure, Handb. Exp. Pharmacol 233 (2016) 173–194. [PubMed: 26578523]

[52]. Morrison SF, Nakamura K, Central mechanisms for thermoregulation, Annu. Rev. Physiol 81 (2019) 285–308. [PubMed: 30256726]

[53]. Herman JP, Mueller NK, Role of the ventral subiculum in stress integration, Behav. Brain Res 174 (2) (2006) 215–224. [PubMed: 16876265]

[54]. Cooper DC, Klipec WD, Fowler MA, Ozkan ED, A role for the subiculum in the brain motivation/reward circuitry, Behav. Brain Res 174 (2) (2006) 225–231. [PubMed: 16870273]

[55]. Cui H, Mason BL, Lee C, Nishi A, Elmquist JK, Lutter M, Melanocortin 4 receptor signaling in dopamine 1 receptor neurons is required for procedural memory learning, Physiol. Behav 106 (2) (2012) 201–210. [PubMed: 22342812]

[56]. Kelley AE, Ventral striatal control of appetitive motivation: role in ingestive behavior and reward-related learning, Neurosci. Biobehav. Rev 27 (8) (2004) 765–776. [PubMed: 15019426]

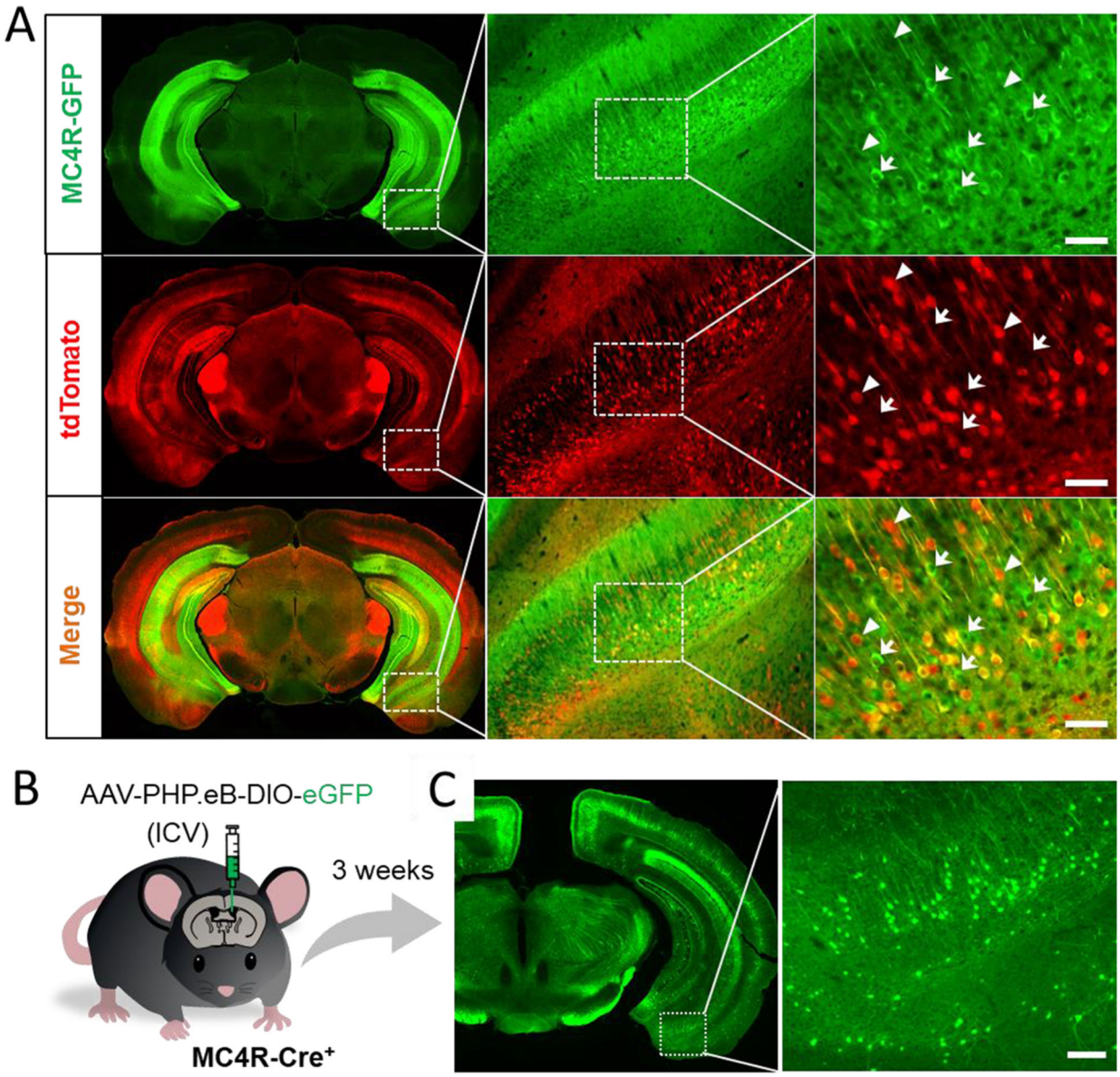

Fig. 1.

MC4R expression in the vSUB. (A) Representative images showing GFP and tdTomato in the vSUB of MC4R-GFP/MC4R-Cre/tdTomato triple transgenic mice. Note partially mismatched labeling of GFP and tdTomato in the vSUB; white arrows indicate GFP+ but tdTomato-neurons (ectopic expression of MC4R-GFP) and white arrowheads indicate GFP- but tdTomato+ neurons. (B) Schematic showing ICV injection of AAV into MC4R-Cre+ mouse. (C) Representative images showing MC4R-expressing (GFP+) neurons in the vSUB. Scale bar, 50 um for A and 100 um for C.

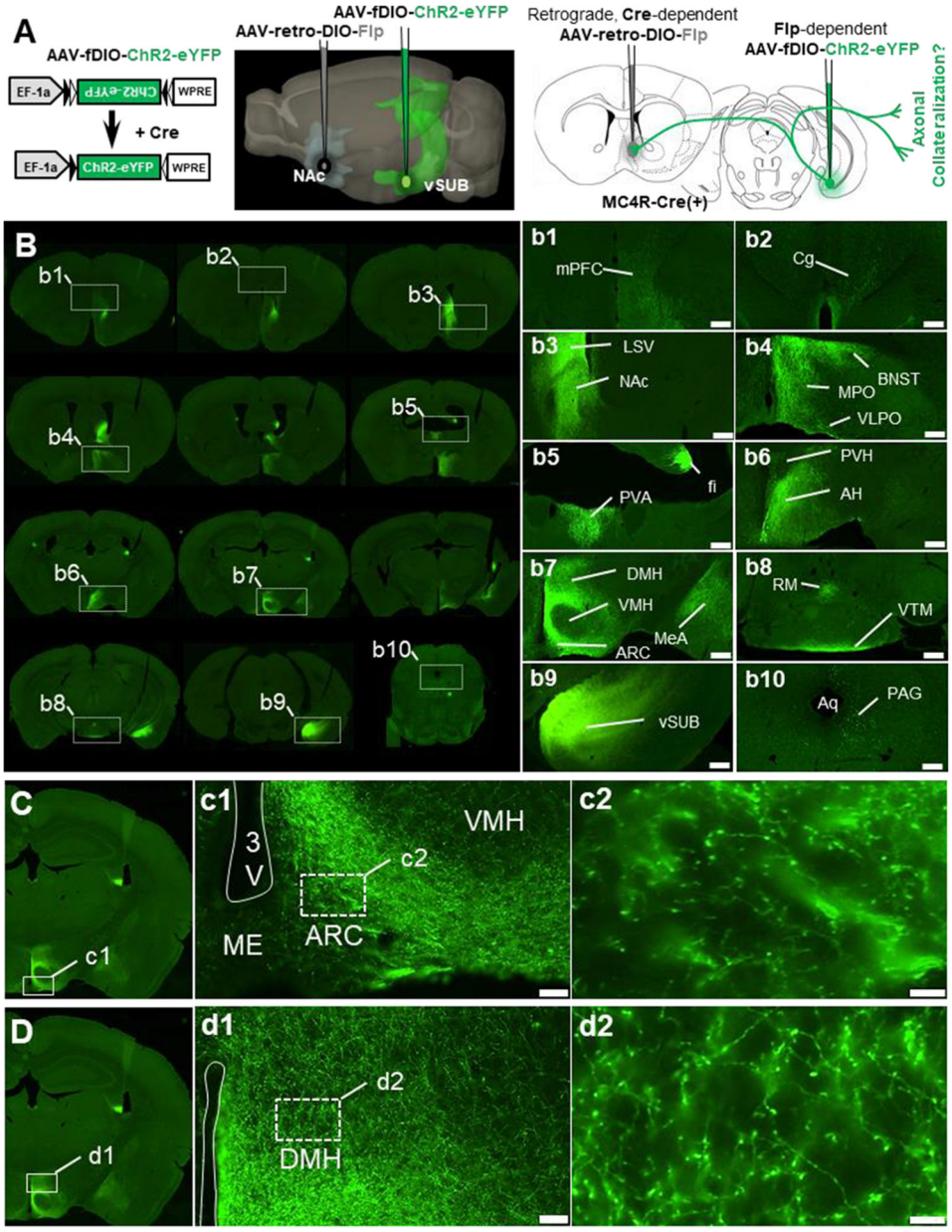

Fig. 2.

Viral-mediated cell type (*MC4R*)- and circuit (NAcSh)-specific anterograde tracing reveals extensive collateral projections of vSUB^{MC4R+} neurons. (A) Schematic showing a combination of viral injection into the NAcSh and the vSUB. (B) Representative images of brain sections showing collateral projections of vSUB^{MC4R+} neurons to different brain regions. (C, D) Zoom-in images in ARC (C) and DMH (D) showing eYFP puncta resembling synaptic boutons. (E) The summary of innervated brain regions. The density of GFP fibers is estimated and indicated as sparse (+), moderate (++), dense (+++), heavy (++++) and compact (+++++). 3v, third ventricle. Scale bar, 200 μm for b1-b10; 50 μm for c1 and d1; 10 μm for c2 and d2.

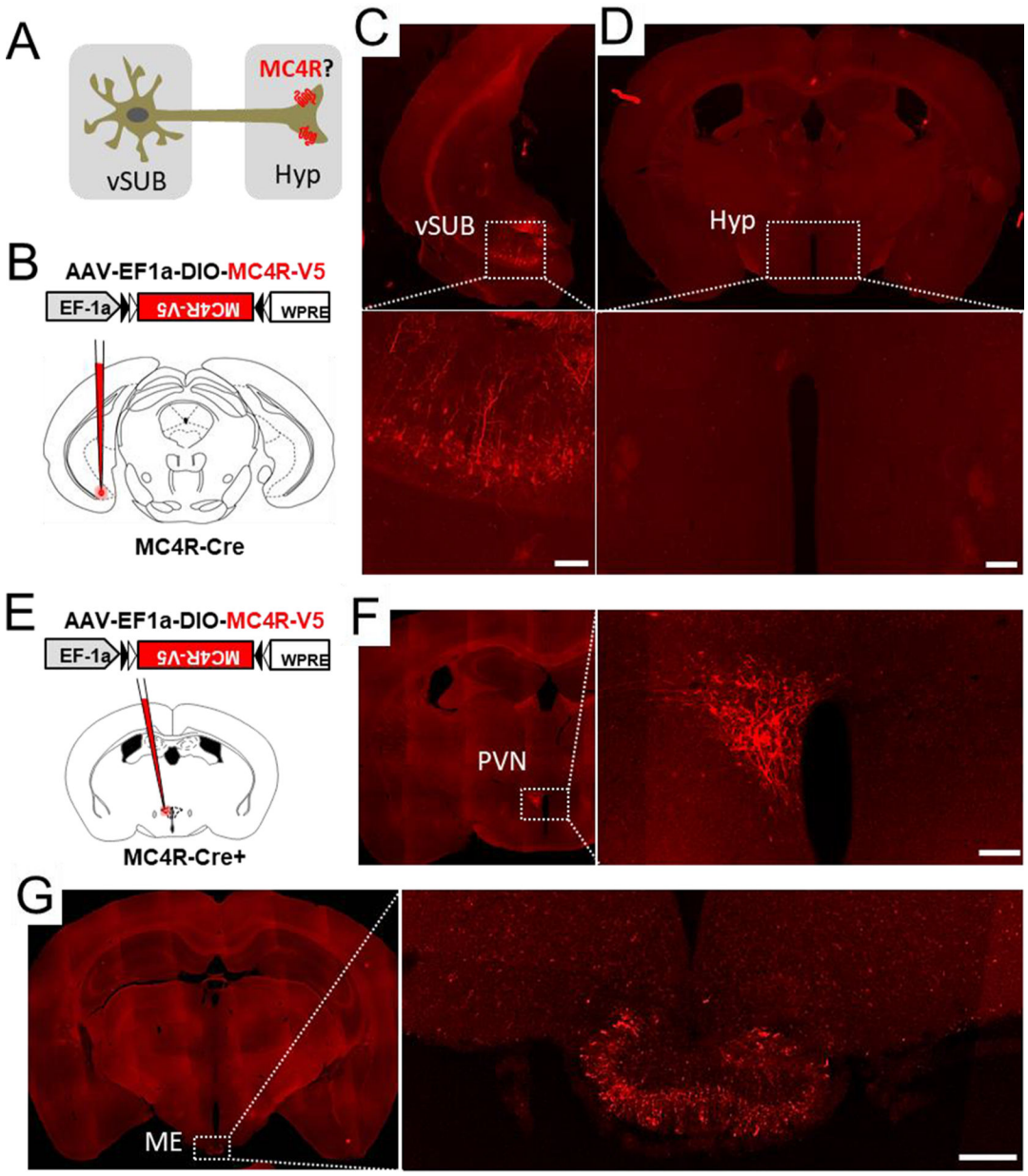

Fig. 3.

MC4Rs do not localize to presynaptic axon terminals of vSUB neurons in the hypothalamus. (A) Schematic showing a hypothesis of presynaptic model of MC4R to be tested. (B) Schematics showing microinjection of Cre-dependent AAV-DIOMC4R-V5 into the vSUB of MC4R-Cre mice. (C) Representative images showing overexpression of MC4R-V5 in the vSUB. (D) Representative images showing that MC4R-V5 is undetectable by V5 immunostaining in the hypothalamus. (E) Schematics showing unilateral microinjection of Cre-dependent AAV-DIO-MC4R-V5 into the PVN of MC4R-Cre mice. (F) Representative images showing overexpression of MC4R-V5 in the PVN. (G) Representative images showing that presynaptic axon terminal localization of MC4R-V5 in PVN MC4R+ neurons. Scale bars, 100 um.

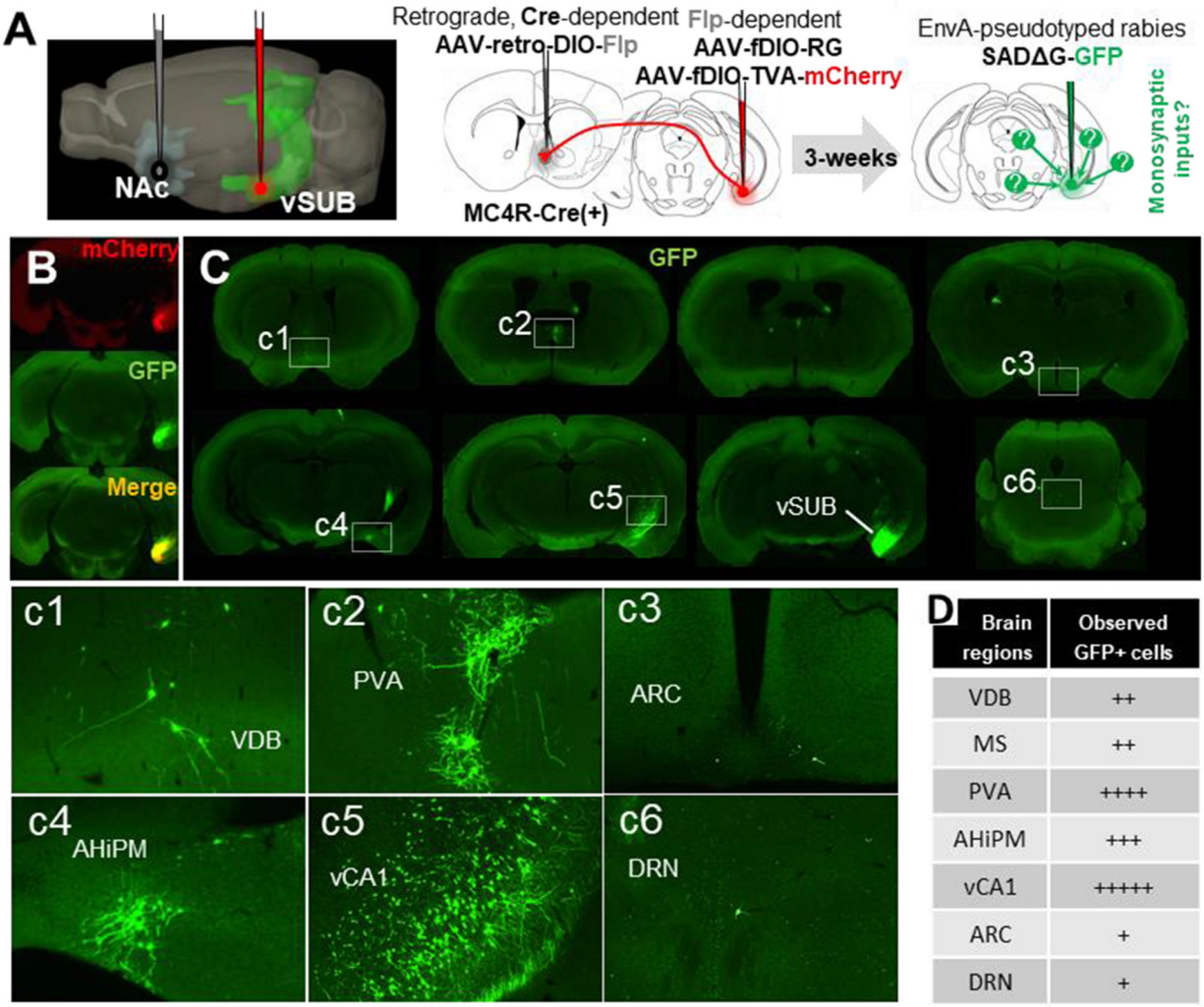

Fig. 4.

Brain-wide mapping of monosynaptic inputs to NAcSh-projecting vSUB^{MC4R+} neurons by cell type-specific Tracing Relationships between Input and Output (cTRIO). (A) Schematic showing a combination of viral injection into the NAcSh and the vSUB for cTRIO. (B) Representative images showing precise targeting of TVA-mCherry and SADΔG-GFP into the vSUB. (C) Representative images of brain sections showing the brain regions sending monosynaptic inputs to NAcSh-projecting vSUB^{MC4R+} neurons. (D) The summary of brain regions where GFP+ cells are observed. The density of GFP+ cells is estimated and indicated as sparse (+), moderate (++), dense (+++), heavy (++++) and compact (+++++). Scale bar, 100 μm.

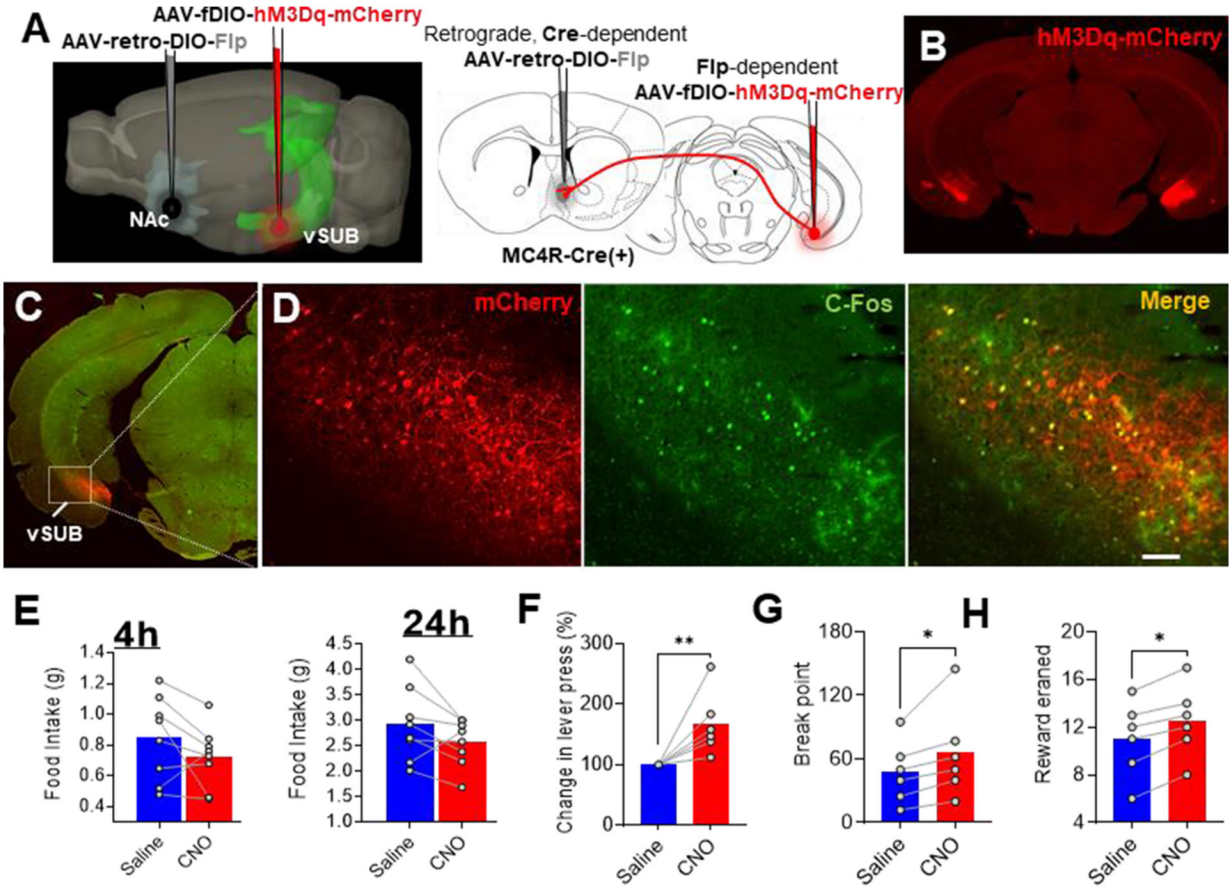

Fig. 5.

The effects of chemogenetic activation of NAcSh-projecting vSUB^{MC4R+} neurons on feeding and food motivation. (A) Schematic showing a combination of viral injection into the NAcSh and the vSUB for DREADD activation of NAcSh-projecting vSUB^{MC4R+}neurons. (B) Representative image showing bilateral expression of excitatory DREADD receptor hM3Dq-mCherry in the vSUB. (C, D) Representative image showing effective activation of NAcSh-projecting vSUB^{MC4R+} neurons by CNO (2 mg/Kg) as shown by c-Fos expression in mCherry+ neurons. (E) The effect of acute DREADD activation of NAcSh-projecting vSUB^{MC4R+} neurons on food intake. (F-H) Total number of lever presses (F), break point (G), and total number of rewards earned during PR test (H). Scale bar, 100 μm. *$p < 0.05$, **$p < 0.01$ by paired t-test.

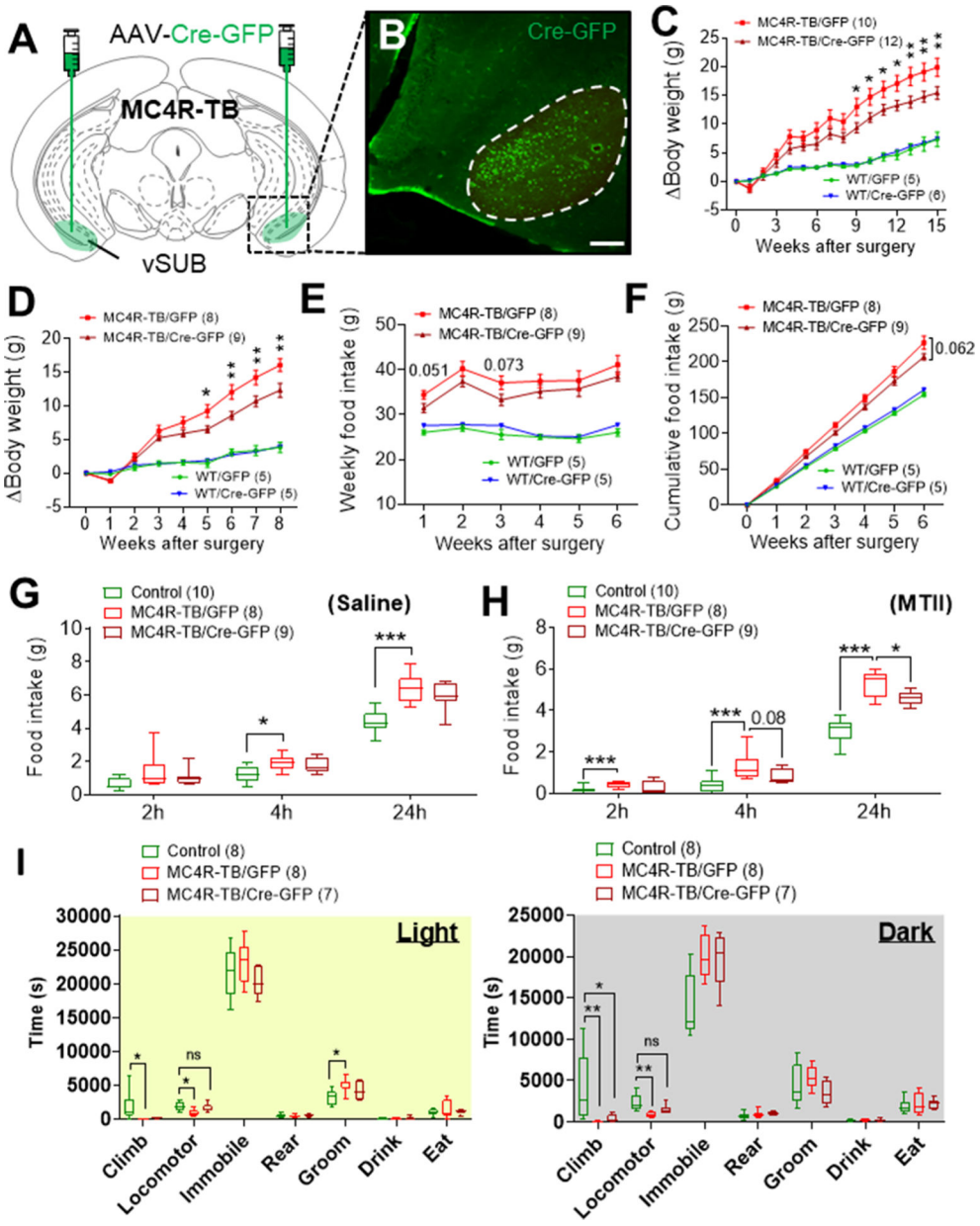

Fig. 6.

The effects of restoration of vSUB^{MC4R} signaling on body weight, food intake and home cage behaviors. (A, B) Schematic showing bilateral injection of viral vector into the vSUB of *MC4R*-TB mouse (A) and representative image showing the precise targeting of AAV-Cre-GFP into the vSUB (B). (C) Body weight change in a cohort of 10-week-old mice received AAV injection into the vSUB. (D-F) Body weight change (D), weekly (E) and cumulative (F) food intake in an additional cohort of singly housed 8-week old mice received AAV injection into the vSUB. (G, H) Cumulative food intake in singly housed mice received either saline (G) or *MC4R* agonist MTII (2 mg/Kg) (H) at the onset of dark cycle (6 PM). (I) Home cage behaviors measured by LABORAS system. Scale bar, 200 μm.

*$p < 0.05$, **$p < 0.01$, ***$p < 0.001$ by either RM of two-way ANOVA (C–H) or one-way ANOVA (I). Data are presented as mean ± SEM.

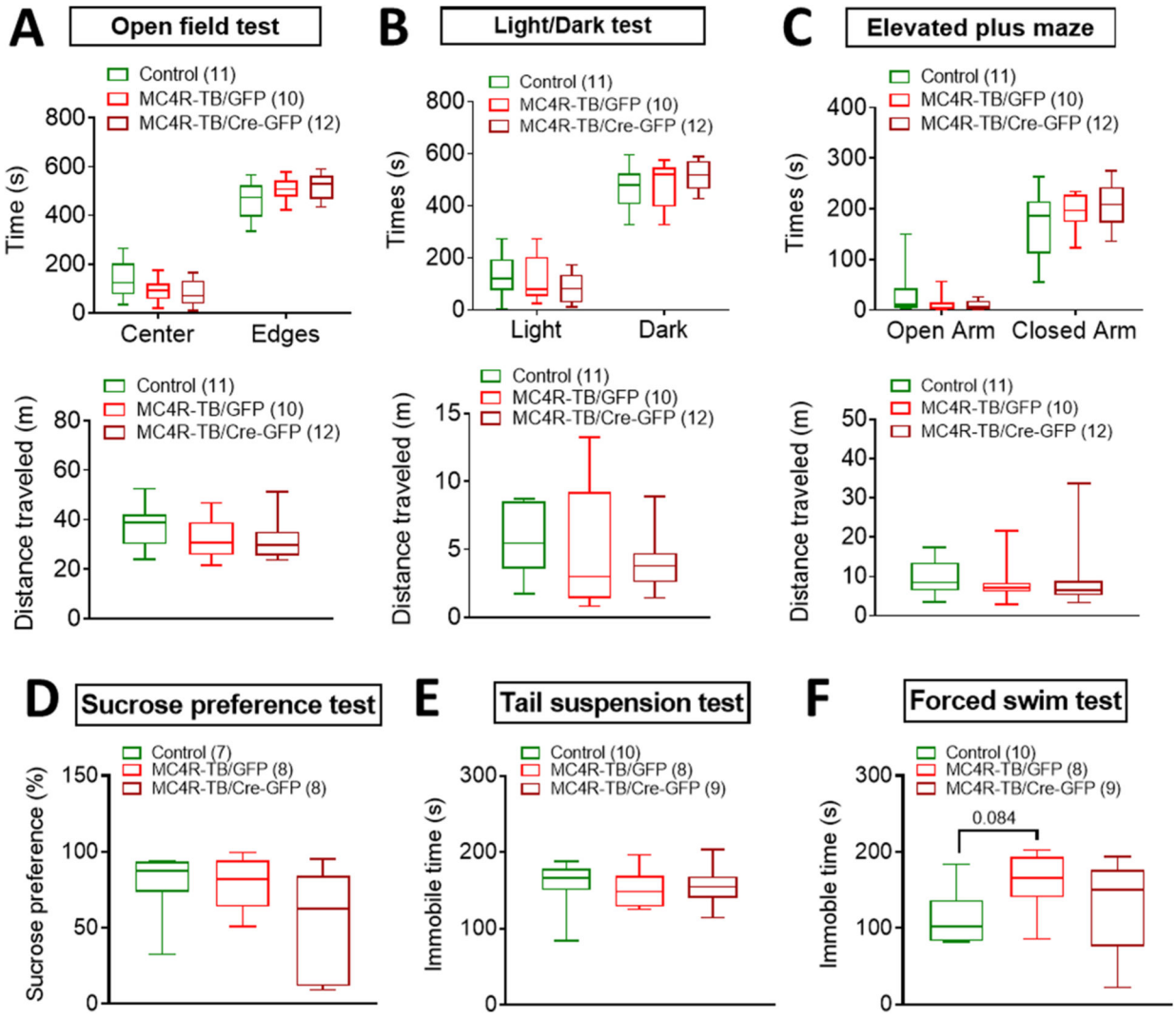

Fig. 7.

The effects of restoration of vSUB^{MC4R} signaling on anxiety- and depression-like behaviors. (A) Time spent in center and edges and distance traveled during open field test. (B) Time spent in light and dark boxes and distance traveled during light/dark box test. (C) Time spent in open and closed arms and distance traveled during elevated plus maze test. (D) Preference of sucrose over water during sucrose preference test. (E) Immobile time during tail suspension test. (F) Immobile time during forced swim test.